

A technoeconomic assessment of microalgal culture technology implementation for combined wastewater treatment and CO₂ mitigation in the Arabian Gulf

Ahmed M.D. Al Ketife¹, F. A. O. Al Momani^{2*}, Muftah EL-Naas¹, Simon Judd^{1,3},

¹Gas Processing Center, Qatar University; ²Department of Chemical Engineering, Qatar University; ³Cranfield Water Science Institute, Cranfield University,

*corresponding author

Abstract

A technoeconomic assessment (TEA) has been conducted of the feasibility of large-scale application of microalgal culture technology (MCT) to the combined mitigation of CO₂ emissions from flue gases and nutrient discharges from wastewater in the Arabian Gulf. The assessment has incorporated the selection of the algal species and MCT technologies, the extent of nutrient removal, and the biomass/biofuel production rate. The cost benefit of the abatement of pollutants (in the form of CO₂ and nutrient discharges) was included by assigning appropriate credits to these contributions. The overall economic viability was quantified as the break-even selling price (BESP) of the generated biocrude, taken to be the price at which the product must sell to cover the operating expenditure (OPEX). Based on available information and optimal operational conditions, the BESP was calculated as being \$0.544 per kg biomass, equating to \$0.9 L⁻¹ for the extracted biocrude, the credited items contributing ~14% of this figure. The BESP was found to be most sensitive to the algal growth rate μ , the BESP changing by $\pm 24\%$ in response to a $\pm 20\%$ change in μ . Whilst the terms of reference of the study are limited to OPEX contributors, the potential for sustainability associated with the innately reliably high levels of natural light in the Gulf region appear to provide auspicious circumstances for large-scale implementation of MCT. For emerging economies with a comparable climate but without a mineral oil-based economy a greater financial benefit from the proposed scheme would arise.

Keywords: *Technoeconomic analysis; Microalgae culture technology; break-even selling price; large-scale implementation; carbon dioxide biofixation; nutrient removal.*

Abbreviations

APR	Algal pond reactor
AST	Abiotic sewage treatment
BESP	Break-even selling price with reference to OPEX
BSDP	Biomass solar drying process
CPC	Solar-tracking compound parabolic collector
CSO	Combined sewer overflow
fte	Full-time equivalent
GWP	Green wall panel
HTL	Hydrothermal liquefaction
IWPP	Integrated water and power plant
MCT	Microalgae culture technology
OPEX	Operating expenditure
PBR	Photobioreactor
TEA	Technoeconomic analysis
TPP	Thermal power plant
TSS	Total suspended solids
WwTW	Wastewater treatment works

Symbols

h_{co}	Combustion energy of algae biomass, J Kg ⁻¹
ϵ	Emissivity of the water in the infrared region, -
A	Pond surface area, m ²
IC	Inorganic carbon concentration, mg L ⁻¹
Co	Cost of MCT biomass production per unit biomass, \$ kg ⁻¹
Cp	Growth medium heat capacity, J kg ⁻¹ °K ⁻¹
Cr	Credit from relevant MCT-related parameter per mass of biomass produced, \$ kg ⁻¹
C_s	Saturation concentration of CO ₂ , mg L ⁻¹
D_C, D_o	Diffusivity of CO ₂ , oxygen, m ² .s ⁻¹
d_{th}	Biomass loss (death) rate, d ⁻¹
$E_{biocrude}$	Biocrude energy content, MJ kg ⁻¹
$E_{petroleum}$	Petroleum energy content, MJ kg ⁻¹
E_{vr}	Rate of evaporation, kg hr ⁻¹
f_b	Daily photoperiod, d
f_{Xoil}	Potential extractable oil content of dry basis, % w/w
hc	Heat transfer coefficient, W m ⁻²
$H_{C,o}$	Henry constant for O ₂ or CO ₂ , D.L
I_0	Incident light, µE m ⁻² s ⁻¹
I_{av}	The average irradiance, µE m ⁻² s ⁻¹
I_d	Daily total light intensity at pond surface, µE m ⁻² s ⁻¹
I_S	PAR half saturation constant, µE m ⁻² s ⁻¹
I_t	Total light intensity, µE m ⁻² .s ⁻¹
K_c	Chlorophyll-base light extinction coefficient of algae, cm ² (mg Chl-a).
k_C, k_O	Mass transfer coefficient of CO ₂ , oxygen, d ⁻¹
K_i	Half saturation constant for nutrient i , -
K_{ih}	Self-inhibition constant, mg L ⁻¹
K_L	Light extinction coefficient, g m ⁻²
MW_i	Molecular weight of species i , g mol ⁻¹
n	Shape factor, -
p	Pressure, bar
P_a	Areal biomass productivity, kg m ⁻² d ⁻¹
PAR	Photosynthetically active radiation, µE m ⁻² s ⁻¹
P_v	Volumetric productivity, kg m ⁻³ d ⁻¹
P_X	Annual biomass productivity, tn y ⁻¹

Q_i	Energy loss or gained, W
q_m	Maximum specific transformation rate, d ⁻¹
R	Universal gas constant, L ³ bar ⁻¹ K ⁻¹ mol ⁻¹
S_i	Concentration of selected nutrient, mg L ⁻¹
OC	Organic carbon concentration, mg L ⁻¹
TP	Total phosphorus concentration, mg L ⁻¹
TN	Total Nitrogen concentration, mg L ⁻¹
C, c_g	Gas concentration, %
T	Temperature, °K
t	Time, days
T_a	Air temperature, °K
T_s	Ambient temperature for clear sky days, °K
T_w	Temperature of cultivation media, °K
V	Volume, L
X	Biomass concentration, g L ⁻¹
X_{max}	Maximum biomass concentration, g L ⁻¹
W_i	Molecular weight of species i, g mol ⁻¹
y	Mole fraction of CO ₂ in gas phase, -
Y	Yield coefficient for total carbon, g _c g _x ⁻¹
Y_{O_2}	Oxygen yield coefficient, g _{biomass} g _i ⁻¹
z	Pond depth, m
Z	Mass of biomass needed to produced 1 m ³ biofuel of algal biomass, kg
$\gamma_{w,i}$	Half saturation constant for i nutrient, -
ε	Gas holdup volume, L
μ_{max}	Maximum specific growth rate, d ⁻¹
ρ	Density of the cultivation medium, kg m ⁻³
ρ_{oil}	Biocrude density, kg m ⁻³
σ	Stefan–Boltzman constant, W m ⁻² °K ⁻⁴

Subscripts

g	Gas phase
i	Substrate/nutrient (OC, N, P)
l	Liquid phase
tot	Total concentration
R	Reactor
$init$	Initial value
atm	Atmospheric
$feed$	Feed

1 Introduction

Carbon dioxide (CO₂) fixation methods are well known, and include its conversion to chemical feedstock and fuels, biological conversion (photosynthesis) (Al Momani et al., 2004), and mineralisation for the production of metal carbonate/bicarbonates (Almomani et al., 2019a; Almomani et al., 2019b; Laumb et al., 2013). Whereas these methods mainly focus on CO₂ utilisation following capture, biological conversion directly mitigates CO₂ and uses it as a feedstock to create useful products.

Microalgae are acknowledged as providing an efficient means of mitigating carbon while generating products such as biofuels (Almomani et al., 2019a; Meher et al., 2006; Mutanda et al., 2011); interest in microalgae culture technology (MCT) has grown significantly since first it was pioneered in the late 1970s (Leduy and Therien, 1979). Algae can utilise both CO₂ and organic carbon as the substrate, by autotrophic and mixotrophic growth respectively, such that the

technology can potentially be employed for combined CO₂ sequestration from flue gases and nutrient removal from wastewater (Almomani et al., 2017; AlMomani and Örmeci, 2016; Shurair et al., 2016; Almomani et al., 2014). Whilst the economics of this option are not normally favourable (Judd et al., 2017; Mohamad et al., 2017), the sub-tropical climate of the Arabian Gulf, where there is an abundance of natural light, makes MCT closer to being viable in this region than in less temperate zones

The paper sets out to establish the technical feasibility and quantify the cost benefit of a sustainable MCT- based carbon capture and wastewater treatment scheme for implementation in a warm, arid climate. In this regard its specific most novel elements comprise:

- a) Selection of the corresponding most appropriate algal species, though reference to available information.
- b) Maximising the harnessing of solar energy, both for (i) promoting algal growth, and (ii) disinfecting the clarified municipal wastewater source, the latter providing an additional cost benefit through obviating conventional wastewater treatment.
- c) Implementation at national scale with due consideration of the regional ambient conditions.

Only two other examples have been published in this specific area (Hernández-Calderón et al., 2016; Orfield et al., 2014), neither of which encompass the novel sustainable design elements proposed in the current study.

2 Species selection

The microalgal strain selected for MCT must be robust to the prevailing environmental conditions, but also have a rapid growth rate and a high yield of the cell materials forming the biofuel product. For the envisaged application both the APR and PBR (algal pond and photobioreactor) configurations are considered, and the boundary conditions determined by wastewater quality and CO₂ gas concentration. Growth under both mixotrophic and autotrophic conditions is required, permitting the removal of both CO₂ and dissolved organic carbon from the wastewater as well as the key nutrients of nitrogen (N) and phosphorus (P). The environmental conditions are set by the water salinity and temperature conditions, demanding thermal tolerance.

A review of the available information suggests the species *Nannochloris* sp. as being appropriate. This strain has featured in published studies elsewhere (Table 1). Whilst peer-reviewed studies of the species have been limited (Fig. 1), it has been locally identified and selected via ribotyping (a molecular technique for bacterial identification and characterization that uses information from rRNA-based phylogenetic analyses), and its growth rate and lipids production rate determined following the screening of 55 species (Saadaoui et al., 2016).

The strain is reported to be tolerant to a 50-950 μ E light intensity range (Jazzar et al., 2015; Saadaoui et al., 2016; Takagi et al., 2000; Teo et al., 2014; Wahidin et al., 2013), a broad (0.03 - 80%) CO₂ gas concentration range (Liu et al., 2013; Watanabe and Fujii, 2016), a pH range of 7-9 (Kim and Lee, 2016) and salinities up to 10 g L⁻¹. Its oil content has been reported to be between 31 and 40% with a triacylglycerol (TAG) content up to 21% (Jazzar et al., 2015; Li et al., 2014; Stepan et al., 2016; Takagi et al., 2000; Teo et al., 2014; Wahidin et al., 2013). The biomass concentration range is 20-60 kg/m³ for a PBR (Wileman et al., 2012), the growth phase relatively short at 4 days (Jiménez-Pérez et al., 2004; Saadaoui et al., 2016) and the growth rate relatively

high at 1.32 d⁻¹ (Ishika et al., 2017). The species is tolerant to N and P concentrations up to 100 and 500 mg L⁻¹ respectively (Jiménez-Pérez et al., 2004), and hydraulic retention times (HRT) of 6-24 hrs⁻¹ validated (Terigar and Theegala, 2014) with growth under the mixotrophic conditions of wastewater treatment confirmed (Stepan et al., 2016) (Table 1).

Figure 1
Table 1

3 Model development

3.1 Substrate fixation and assimilation

The molar balance for dissolved inorganic carbon of concentration (C) in a completely mixed liquid phase of reactor volume (V), and gas hold-up volume ε over time (t , days) is:

$$(1 - \varepsilon)V \frac{dc}{dt} = M_t - M_c \quad (1)$$

where M_t , the rate of CO₂ transferred from gas to liquid phase, is represented by dual-film theory (Cabello et al., 2014):

$$M_t = k_c (C_s - C)V(1 - \varepsilon) \quad (2)$$

M_c is the rate of CO₂ uptake by the biomass, expressed in terms of the change in biomass concentration dX , the algal biomass yield per unit carbon Y , and the molecular weight of bicarbonate W_{HCO_3} :

$$M_c = V(1 - \varepsilon) \left(\frac{1}{Y} \right) \left(\frac{dX}{dt} \right) \left(\frac{1}{W_{HCO_3}} \right) 1000 \quad (3)$$

where k_c is the mass transfer coefficient for the transfer of CO₂ from the gas to bulk culture phase and C_s is the saturated concentration of CO₂. According to Henry's law:

$$C_s = \frac{py}{RTH_e} W_{HCO_3} 1000 \quad (4)$$

where p is the pressure, y the gas phase CO₂ fraction, R the gas constant, T the temperature and H_e the Henry's Law constant. k_c can be interpolated from correlations available (Shah et al., 1982) for the oxygen transfer coefficient k_o using the aqueous phase diffusivities of CO₂ and O₂ (D_c and D_o respectively):

$$k_c = k_o \sqrt{\frac{D_c}{D_o}} \quad (5)$$

ε in Eq. 3 is estimated by volumetric expansion (Chisti, 2007) based on the gassed and un-gassed height of fluid (h_G and h_L respectively) in each part of the reactor:

$$\varepsilon = \frac{h_G - h_L}{h_G} \quad (6)$$

The mass balance for total dissolved nutrients (N and P) not involved in the gas liquid mass transfer phenomena can be expressed as:

$$\frac{dC_{N,P}}{dt} = -1000Y_{N,P} \mu_X X \quad (7)$$

with appropriate initial conditions of:

$$[N, P] = [N_{init}, P_{init}] \text{ at } t=0 \quad (8)$$

The dissolved organic matter biodegradation rate is described by the Haldane equation (Anderson et al., 2002):

$$-\frac{d(s)}{d(t)X} = \frac{q_m S}{K_s + S + S^2 / K_{ih}} \quad (9)$$

where t is the time (days), X the biomass concentration, S the organic matter concentration (mg L^{-1}), q_m the maximum specific transformation rate. K_s and K_{ih} are the half saturation coefficient and the self-inhibition constant (mg L^{-1}) respectively.

3.2 Biomass growth

The general logistic model can be used to predict growth rate of algal biomass dX/dt :

$$\frac{dX}{dt} = \mu_x X \left(1 - \frac{X}{X_{\max}}\right) - d_{th} X \quad (10)$$

where μ_x is the specific growth rate in d^{-1} , X_{\max} the maximum biomass concentration reached during the cultivation period, and d_{th} the biomass death rate.

The integrated Monod model correlating the algal specific growth rate with substrate concentration and light intensity has been proposed by (Bernard et al., 2001), extending Equation 10:

$$\mu_x = \mu_{\max} \left(\prod_i^N \left[\frac{N_i}{K_i + N_i} \right] \right) \left[\frac{q_m S}{K_s + S + S^2 / K_{ih}} \right] \left[\frac{I_{av}^n}{I_s^n + I_{av}^n} \right] [T_{(T)}] \quad (11)$$

where N_i represents the respective N, P and total C content of the culture, K_i the corresponding half saturation constants for substrate or nutrient i , and I_s the corresponding parameter for light. The average radiant energy I_{av} within the bulk culture medium is estimated assuming exponential decay of the radiant energy I_0 at the incident reactor surface. For a completely mixed liquid phase, the average light intensity for the culture volume is given by (Sciandra, 1986):

$$I_{av} = \frac{1}{z} \int_0^z I_0 \exp(-K_L \tau) d\tau \quad (12)$$

where z is the pond depth and K_L the overall light extinction coefficient. Generally, light intensity decreases exponentially with distance from the reactor wall due to the increase in algal cell concentration:

$$\frac{I_{av}}{I_0} = \exp(-K_L L) \quad (13)$$

where K_L is correlated with the algae concentration (X_A) (Jupsin et al., 2003):

$$K_L = f(X_A) \quad (14)$$

The diurnal variation of the surface light intensity, I_0 , can be estimated assuming a sinusoidal function for the photoperiod (Smith, 1980):

$$I_0(t) = \left(\frac{\Pi I_d}{2 f_p} \right) \sin \left(\frac{\Pi t}{f_p} \right) \quad (15)$$

where I_d is the total daily light intensity at the pond surface and f_p the fraction of the photoperiod in a day.

The influence of temperature is accounted for by (Stewart, 2005):

$$T_{(T)} = 0.06^{(T-20.035)} \quad (16)$$

In a batch process operation, the volumetric productivity (P_v in $\text{kg m}^{-3} \text{d}^{-1}$) for the biomass is given by:

$$P_v = \frac{X_{\max} - X_{\text{init}}}{\Delta t} \quad (17)$$

where X_{init} is the initial biomass concentration in kg m^{-3} and Δt the time interval between inoculation and the maximum biomass concentration.

The areal biomass productivity, P_a in $\text{kg m}^{-2} \text{d}^{-1}$, of an APR can obtained from the volumetric productivity:

$$P_a = P_v L \quad (18)$$

The combined set of ordinary differential equations (*ODEs*) were coded in MATLAB to combine the time-dependent algal biomass concentration X (g L^{-1}) and algal nutrient uptake functions with light intensity, and the simulations validated with the experimentally-determined C_v growth data. A sensitivity analysis (σ_x) of an examined parameter P_j was conducted with respect to X to assess the response of biomass concentration to changes in each model parameter:

$$\sigma_x = \frac{\Delta X}{\Delta P_j} \frac{P_{j\text{nom}}}{X_{\text{nom}}} \quad (19)$$

where $P_{j\text{nom}}$ is the parameter nominal value and X_{nom} the model response using the nominal parameter values. A $\pm 20\%$ variation in ΔP_j was applied to obtain the test values to determine ΔX . Four biomass profiles were used in calculating the mean profile with the standard deviation estimated from the four profiles. The sensitivity coefficient for each parameter was calculated from the average spread according to published methods (Bernard et al., 2001; Lardon et al., 2009). An F-test was performed to determine the variance between the predicted and measured values using the *Imp* statistical discovery software (*SAS version 11.2.1*).

3.3 MCT process facets

A novel abiotic sewage treatment (AST) process is to be used for wastewater pre-treatment prior to a set of green wall panels (GWPs) and APRs, the GWPs being used to produce the inoculum while mass production is carried out in the APRs. Subsequent stages comprise algal harvesting followed by hydrothermal liquefaction (HTL) extraction of bio-crude, followed by bio-oil production (Fig. 2).

The AST process is intended to remove suspended matter prior to disinfection by UV irradiation, disinfection being required to avoid contamination of the algal culture (Qadir et al., 2010). Clarification is needed to ensure reasonable UV transmittance and so sufficient disinfection capacity (Agulló-Barceló et al., 2013); the target TSS UV unit inlet total suspended solids (TSS) concentration is thus 90-100 mg L⁻¹.

Solar-tracking compound parabolic collectors (CPCs) are used to supply solar energy for both the UV unit and the biomass solar drying process (BSDP). Water is evaporated by concentrating the solar energy using the CPCs to provide a slurry of 20% solids to feed to the HTL process. An APR HRT of two days is required to achieve a 0.5 Kg cell density per m³.

3.1 Greenhouse design

The greenhouse for the APR is to be constructed of white polypropylene material (Kmart Australia Limited, Australia) intended to filter the light to a specific wavelength to promote biomass productivity (Almomani et al., 2017; Shurair et al., 2016; Znad et al., 2018a; Znad et al., 2018b). The cover also reduces the water evaporation rate and risk of contamination, but then demands temperature control. The latter is to be achieved through natural convection in the head space between the APR and CT.

A simple thermal energy balance can be conducted across the APR to assess the influence of radiation, evaporation, and convection on the medium temperature, assuming:

1. APR is a shallow pond with no temperature gradient in the cultivation medium.
2. The APR walls are completely insulated such that heat loss through walls is negligible.

3.1.1 APR heat balance

The thermal energy balance across the APR greenhouse is represented by the following equation:

$$\rho CpAz \frac{dT}{dt} = Q_{irradiance} - Q_{absorbed} - Q_{radiation} - Q_{evaporation} - Q_{convection} - Q_{conduction} \quad (20)$$

where ρ (kg m⁻³) is the cultivation medium density, A (m²) the pond surface area, Cp (J kg⁻¹ °K⁻¹) the growth medium heat capacity, z (m) the pond depth, $Q_{irradiance}$ the solar heat flow (or power) to the pond, $Q_{absorbed}$ the solar power to the algal cells during growth, $Q_{radiation}$ the power emitted by radiation, $Q_{evaporation}$ the power associated with either condensation or evaporation, $Q_{convection}$ the convective heat loss, and $Q_{conduction}$ the heat flow between the pond and the ground (Andersen, 2005; Huesemann et al., 2018) - assumed negligible, Q being in Watts.

The cultivation medium is heated by solar irradiation entering the culture volume:

$$Q_{irradiance} = AI_t \quad (21)$$

I_t (μE m⁻²s⁻¹) is the total light intensity received by the pond, part of which is used for photosynthesis by the microalgae cells:

$$Q_{absorbed} = h_{co}\mu_{max}XV \quad (22)$$

$Q_{absorbed}$ is a function of the combustion energy of the algae biomass h_{co} (J Kg⁻¹), the growth rate μ_{max} (s⁻¹), the biomass concentration X (kg m⁻³) and the pond volume V (m³). The pond water emits thermal energy as longwave radiation (Duffie and Beckman, 2013):

$$Q_{radiation} = A \epsilon \sigma ((T_W^4 + 273.15) - T_s^4) \quad (23)$$

where ϵ (dimensionless) is the emissivity of the water in the infrared region, σ (W m⁻² K⁻⁴) the Stefan–Boltzman constant and T_s the ambient temperature for clear sky days (Duffie and Beckman, 2013).

Evaporation is the most influential parameter on the medium temperature, especially in a location with low average humidities. Evaporative losses can be calculated from:

$$Q_{evaporation} = \Delta H E_{vr} \quad (24)$$

where E_{vr} (kg hr⁻¹) is the rate of evaporation, which can be given by:

$$E_{vr} = 2.06 \times 10^3 A (P_W - P_a) \quad (25)$$

and ΔH (KJ Kg⁻¹) is the heat of evaporation for water.

Convection causes heat loss as a result of replacing the hot rising air near the pond by the cooler ambient air (Rafferty and Culver, 1998):

$$Q_{convection} = h_c A ((T_W + 273.15) - (T_a + 273.15)) \quad (26)$$

h_c (W m⁻²) being the heat transfer coefficient.

3.2 Solar disinfection system: background and design

The proposed MCT employs solar-powered UV irradiation for disinfection of a clarified municipal wastewater source, similar in application to combined sewer overflows (CSOs) (Muller, 2011), and permitting its reuse (Toze, 2006). Reuse of the water for crop irrigation (Briskin, 2000; WHO, 2006), can offset the costly potable water supply produced by seawater desalination, but demands a level of disinfection. The reuse opportunity offered by MCT offers a viable reuse alternative, providing a high-value product (biocrude or biofuel) whilst incurring very low bacteriological risk to human health.

Disinfection upstream of the APR is nonetheless required to maintain the health of the microalgae. The effectiveness of the advocated solar-powered compound parabolic collector (CPC) UV unit has been broadly demonstrated for inactivating a wide range of pathogen microorganisms in water (McGuigan et al., 2012). These devices are inexpensive and low in maintenance, can efficiently concentrate both direct and diffuse solar radiation (Malato et al., 2009), and have been successfully demonstrated for wastewater disinfection (Godwin, 2017). The return of up to 59% (Jones et al., 2014) of the wastewater from the HTL process to the APR would require supplementary treatment, most simply by upgrading the AST process.

The recommended CPC UV device comprises a 4 m-long, 125 mm-diameter borosilicate glass tube (Gaia/OEM model PT-5760, Spain). The parabolic trough solar collector has a reflective surface of 72 m² housed in a galvanized steel frame, with an estimated 20 year life (Ltd, 2017). At an average solar UV irradiance during daylight of 13-50 W.m⁻², the disinfection attained (as log kill, the logarithm of the ratio of the feed to treated water bacterial concentration for a given cumulative UV dose in W.h m⁻² (Breeze, 2016) can be determined.

3.3 Costs equations

The quantity of biomass Z (kg) needed to produced 1 m³ biofuel of algal biomass having a potential extractable oil content of f_{xoil} (% w/w, dry basis) of density ρ_{oil} (kg m⁻³), is given by:

$$Z \cdot f_{xoil} = \rho_{oil} \cdot 1 m^3 \quad (27)$$

such that the amount of biomass required to produce 1 m³ of biofuel is.

$$Z = \frac{\rho_{oil}}{f_{xoil}} \quad (28)$$

The operating expenditure cost (OPEX) is determined by the algae production and oil extraction costs, including the cost of delivery of the wastewater and CO₂ to the MCT, mitigated by the value of the recovered resources such as the biofuel, residual organic carbon (as biogas, for example), and nutrients:

$$B_{co} = Z \times 10^{-3} (C_{Cr} + RN_{Cr} + RP_{Cr} + Fg_{cr} + Ae_{Cr} + BOD_{Cr} - In_{co} - Dfg_{co} - Cf_{co} - Ab_{co} - Dis_{co} - WW_{co} - Sd_{co} - HTL_{co} - Solar_{co} - Pre_{co}) \quad (29)$$

where B_{co} is the biocrude production cost (\$/L), In_{co} is the cost of inoculation, Dfg_{co} the cost of delivered flue gas, Cf_{co} is the cost of cultivation, Ab_{co} is the cost of abiotic WW treatment, Dis_{co} cost of disinfection, WW_{co} cost of delivered WW, Sd_{co} the cost of solar drying, and HTL_{co} the cost of biocrude production. C_{Cr} , RN_{Cr} , RP_{Cr} , Fg_{cr} , Ae_{Cr} , BOD_{Cr} respectively refer to the credit from carbon, N and P removed from the wastewater, from the flue gas, Ae_{Cr} from gas aeration, credit from biological contaminants removal, all costs being in \$/Kg. Substituting Eq. 31 in Eq 32:

$$B_{co} = \frac{\rho_{oil}}{f_{xoil} 10^3} (C_{Cr} + RN_{Cr} + RP_{Cr} + Fg_{cr} + Ae_{Cr} + BOD_{Cr} - In_{co} - Dfg_{co} - Cf_{co} - Ab_{co} - dis_{co} - WW_{co} - Sd_{co} - HTL_{co} - Solar_{co} - Pre_{co}) \quad (30)$$

The above equation can encompass the extracted biomass lipids conversion to biocrude via hydrothermal liquefaction (HTL) and upgrading processes (Zhu et al., 2013). An established parameter in published economic analyses is the break-even selling price (BESP) (Amanor-Boadu et al., 2014), the price for the algal biomass with a given oil content for the equivalent price of crude petroleum yielding the same amount of energy in MJ. This estimated price can then be compared with the total cost of algal biomass production (Eq. 33). The quantity of algal biomass (Z , kg) with the energetic equivalent of a litre of crude petroleum is:

$$Z = \frac{E_{petroleum}}{f_{xoil} y E_{biocrude}} \quad (31)$$

where $E_{\text{petroleum}}$ is ~45 MJ per kg crude oil at a density of 850 kg m⁻³ of crude petroleum and E_{biocrude} is the energy content of the algal oil in MJ per kg. The latter has been reported as being 38 MJ kg⁻¹ at an assumed density of 887 kg m⁻³.

Assuming conversion of 1 L of crude oil to various useable transport energy products costs roughly the same as converting X kg of biomass to bioenergy, the maximum acceptable price that could be paid for the biomass would be the same price of a barrel of crude petroleum. This parameter can be used as the BESP:

$$\text{BESP (\$/L)} = \frac{\text{Price of 1 barrel of petroleum}}{\text{No. of equivalent litre of biocrude}} \quad (32)$$

Moreover, OPEX will include energy, materials, land, maintenance, insurance, loan payments, taxes, and labor.

3.4 Model strategy

The modelling process begins with collation of relevant literature data as relating, wherever possible, to the Arabian Gulf region. The process then proceeds via the study of the combined influence of the key parameters of wastewater and flue gas composition and flows, environmental conditions, and algal strain on algal growth. The outputs of this stage are then used for the economic analysis, which are subsequently reassessed with reference to biomass/biofuel production, nutrient removal, and the input parameters adjusted as required. The process is repeated until reasonable and representative outcomes are obtained (Fig. 3). The iterated outcomes are then (a) subject to a sensitivity analysis of the key process parameters, and (b) compared with those from similar literature studies for other global locations.

3.5 Design criteria

3.5.1 Environmental conditions

Assumptions made in constructing the model comprise:

- The algal culture considered to have the same rheological properties as water.
- The flow pattern at a selected paddle wheel velocity assumed to be turbulent to prevent stratification, improve oxygen stripping and keep the algal biomass suspended;
- Whilst the average monthly evaporation rate is location dependent, a mean value of 0.4 cm day⁻¹ is assumed (Al-Khayat and Jones, 1999; Das et al., 2016; Davis et al., 2016; Delrue et al., 2012; statista, 2016; Sun et al., 2011), yielding a sub-1% evaporative loss of the wastewater fed to the process.
- The seawater salinity assumed to be 4.1 g L⁻¹ on average, compared to reported values of 3.5-4.1 g L⁻¹ at the surface with maximum of 6 g L⁻¹ (Saadaoui et al., 2016).
- The average ambient temperature assumed to be 35°C (Statistics, 2013).
- The annual average rainfall assumed to be 75 mm p.a. (Statistics, 2017; Statistics, 2013);
- A total average monthly insolation assumed to be ~185 kWh m⁻², with 9.5 h daylight on average providing light of 300-800 nm wavelength (Abdallah et al., 2016; Znad et al., 2018a), based on reported direct normal irradiance values of 550 and 925 μE m⁻²s⁻¹ for January and June respectively (Abdallah et al., 2016; Qatar, 2013, 2014), and an average irradiance of 753 μE m⁻²s⁻¹;
- pH levels maintained below 8 by CO₂ dissolution;

- No significant oxygen inhibition;
- No CO₂ or nutrient limitation;
- APR algal cells comprise >80% of culture volume;
- Biofuel productivity determined entirely by the algal cell triglyceride fraction;
- Latent energy from the non-triglyceride fraction of the algal biomass harnessed for electricity generation to displace the mains electricity supply;
- The biomass sustained by the organic carbon in the wastewater during night-time;
- Average wastewater temperature of 25°C (Castillo et al., 2016).

3.5.2 Technology design

APR cultivation systems are considered to incur lower capital costs and energy demand than PBRs (Slade and Bauen, 2013). They are generally constructed as carousels, with vertical walls and a flat base, and culture is continuously mixed and circulated in the APR using a paddlewheel. The pond width/breadth (W/r) ratio is >10 to ensure even flow, monitored by flow meters (Becker, 2007). The wastewater is fed to the paddlewheel at a constant flowrate and algal culture withdrawn (harvested) continuously at the same flow rate. Other key design facets assumed comprise:

- A nutrient-rich wastewater feed, largely obviating the use of a commercial supply of nutrients (N and P);
- The water is recycled to the process from the HTL, following clarification, retaining most of the nutrients;
- ~30% of the water to the process is lost, demanding a make-up water flow of ~60 MLD;
- The pond is assumed to be constructed with raised walls of compacted earth lined with a 1-2 mm thick polymer membrane to minimise leakage;
- The thickness of the APR walls is neglected in calculating the footprint.
- The algal biomass concentration is kept at 0.5 kg m⁻³ to sustain light penetration (Borowitzka, 2005).
- The process is initiated in batch mode and switched to continuous operation once the required biomass concentration is reached;
- The volume of inoculum is assumed to be 10% of the volume of the medium (Rodolfi et al., 2009);
- A working depth of 0.2 m is assumed; the lower depth being preferred to improve light penetration with an ideal surface to volume ratio (1/h) of 3.3 to 4 m⁻¹;
- The paddlewheel-generated mixing velocity, required to maintain sufficient mixing of the APR biomass, is assumed to be a 30 cm s⁻¹ (Vasudevan et al., 2012);
- The facilities are designed in terraces to enable low-energy water system recycling;
- The cultivation system is modelled as a hybrid system of PBRs and ponds;
- The harvesting and dewatering processes comprise (i) natural settling (Huntley et al., 2015), followed by (ii) filter press (Beal et al., 2012; Corporation, 2018; E Wiley et al., 2011), to produce a 20% solids cake;
- The extraction/conversion is based on hydrothermal liquefaction (HTL) (Davis et al., 2014; Zhu et al., 2013) to produce bio-crude (Turton, 1998);
- Batch inoculation is based on a biomass concentration of 8-10 kg m⁻³;
- Two 1250 m² green wall panel GWP modules are used for the inoculation system, based on a total panel surface of 800 m² and a land surface area of 1250 m² generating 52 m³ culture per module (Guccione et al., 2014; Rodolfi et al., 2009).

- The number of full-time equivalent employees required is 125, similar to a previous estimation (Hoffman et al., 2017), paid at the Gulf region rate (Secretariat, 2005) based on a monthly cost of 1340 USD/per full-time equivalent (fte) at 100% overhead.

3.6 Cultivation system input parameters

The targeted biomass production rate is $40,000 \text{ te.y}^{-1}$, or $19 \text{ m L biofuel.y}^{-1}$. The facilities are to be installed on a 1% slope on sandy soil to assist gravity-fed volume transfer, the 3.6 km^2 rectangular site prepared with cut and fill earthworks to create both the ponds and GWP PBRs. The proposed plant has 88 terraces, the upper terrace containing a parking lots, office and laboratory facilities, and the GWP PBRs. Wastewater and CO_2 flue gas is to be supplied continuously from local wastewater and power plants, assumed to be respectively located 4 and 1 km distant from the site. The number of ponds required to satisfy the targeted production capacity is 350 ha, with another hectare assigned to the GWP PBRs and other facilities (Table 2).

Harvesting is conducted every other day, commencing with the lowest main terrace. The algal biomass is then transferred for downstream processing and the treated supernatant wastewater discharged for further use. Once the lowest ponds are emptied, the second-lowest terrace is harvested, and the algal biomass again transferred and the supernatant discharged as before. This cycle is repeated as the harvesting process moves upwards to the higher terraces, with the water being replenished as needed. The daily water demand is roughly $333 \text{ m}^3 \text{ d}^{-1}$.

Table 2

4 Results and discussion

4.1 Model calibration and validation, algal growth

Assumed values for calibration (Table 3) are based on a range of feedwater and gas concentrations taken from four independent published studies (P1-P4) providing relevant experimental data on algal cell concentration X and, for P3 and P4, nutrient removal as residual concentration (TN and TP). The computed dynamic response for X and total nutrients (Fig. 4) indicate a reasonable fit between the experimental data and model. This then determines the most appropriate values for the key algal growth-related parameters (Table 4) for subsequent validation. Data selected for both calibration and validation cover a wide range of input parameters for $C_{c,g}$, I , N , P , and OC concentrations (Tables 3, 5) so as to appropriately reflect the model's ability to predict the biomass profile under different cultivation conditions.

Table 3

Figure 4

The sensitivity of the growth profile σ_x to the range of values of some key system parameter included in Table 5 indicates it to be most sensitive to the maximum specific growth rate μ_{max} (Fig. 6) corroborating outcomes from a number of other MCT studies (Davis et al., 2014). Regression analysis for the experimental and predicted growth profile was subsequently conducted using SAS statistical analysis software (SAS Institute). A high regression number of 0.99 was obtained along with p values below 0.0001 for the all validated points, indicating a significant fit between measured and predicted values in the current model (Fig 7).

Table 4

Table 5

Figure 5

Figure 6

Figure 7

5 Optimisation, energy balance

Based on the data reported in Tables 1, the optimum conditions, providing the maximum algal growth, considered for the energy balance (Section 3.5.1) comprise a temperature T of 25-40°C and a light intensity I of 250-420 $\mu\text{E m}^{-2} \text{s}^{-1}$. *Nannochloris* sp. has been reported to be tolerant to irradiance levels up to 420 $\mu\text{E m}^{-2} \text{s}^{-1}$ (Jazzar et al., 2015) and temperatures up to 45°C (Saadaoui et al., 2016). Therefore, the targeted energy balance aims to reduce the average I from 753 to 420 $\mu\text{E m}^{-2} \text{s}^{-1}$, whilst the average temperature of 35°C is already within optimum range for rapid microalgae cultivation.

The results obtained from the APR greenhouse analysis (Section 5.2.1) reveal there to be no difference between the reported atmospheric average temperature (35°C) and the calculated temperature inside the greenhouse, due to the lower thermal conductivity of the polypropylene cover (Weidenfeller et al., 2004). Furthermore, based on the model generated in Section 5.2, the temperature of cultivation medium increases only from 25°C (Section 5.7.1) to 26°C - still within the optimum temperature range. There is thus no cooling required to counter seasonal changes, based on a maximum transmittance of 33.9% and filtered the wavelength between 750-350 nm with peak at 413 nm for the polypropylene cover for accelerating algal growth (by up to 46%) (Znad et al., 2018a).

6 Solar disinfection and nutrients

The UV dose required to achieve 3-log disinfection has been reported to be 35 mW.cm^{-2} for an associated transmittance of 20-25% (Cairns, 1996; Camp, 1997; Muller, 2011; Wojtenko et al., 2001). This compares with a solar UV dose of 50 minutes producing a 2-3 log reduction of *Escherichia coil* (Amoah et al., 2007), and more comprehensive disinfection of municipal wastewater at an exposure of 3.33 hrs at an average solar UVA irradiance of 38 W m^{-2} (Agulló-Barceló et al., 2013). Therefore, based on the current design, the required time for disinfection has been estimated to be 50 minutes under the irradiance conditions prevailing between 09:00 and 14:00 (Touati et al., 2017).

The calculated feed gas pressure is 1.6 bar for a volumetric CO_2 gas input of 30 $\text{m}^3.\text{hr}^{-1}$ per APR. At this loading carbon limitation would be mitigated (Lundquist et al., 2010). Based on available data for the wastewater specification in the Arabian Gulf region (Al-Naimi, 2002; Mohamad et al., 2017; Shamim Ahmad et al., 1989), initial nutrient concentrations of 20 mg L^{-1} and 10 mg L^{-1} for N and P respectively were selected. The removal efficiencies for N and P were estimated to be 51% and 86% respectively, compared with negligible OC removal, similar to those reported by previous author (Lam and Lee, 2014).

7 Cost analysis

The cost analysis was conducted based on the selected parameters reflecting the process design (Fig. 3) and the governing equations (Section 3.5). The estimated BEBP was based on credit for nutrient removal (C_{Cr} , RN_{Cr} , RP_{Cr}), flue gas fixation (Fg_{Cr}) and flue gas aeration (Ae_{Cr}), with outgoings incurred by inoculation (In_{co}), flue gas and wastewater delivery (Dfg_{Co} and WW_{co}), cultivation (Cf_{Co}), abiotic wastewater treatment (Ab_{Co}), disinfection (Dis_{Co}), solar drying (Sd_{Co}), and HTL (HTL_{Co}), as given in Table 6. The current analysis reveals the nutrient content of the

wastewater to be sufficient to sustain the required biomass concentration of 0.5 kg m^{-3} . Nutrient removal from the wastewater provides a credit of $0.03\text{-}0.25 \text{ \$ kg}^{-1}$ dry biomass for N and P respectively. The cost of CO_2 as a feed reagent is similarly obviated by the use of flue gas.

The estimated cost of the GWP inoculation system advocated is $0.36 \text{ \$ kg}^{-1}$ dry biomass (Table 9), in keeping with reported data of significantly higher costs for PBR inoculating systems compared with those of the APR (Davis et al., 2011). The next highest estimated cost contribution is the cultivation cost of $0.09 \text{ \$ kg}^{-1}$ dry biomass. It has been reported that, for the cultivation phase in raceway ponds, the most significant component of the energy demand is the recirculation energy, contributing 22%-79% of the total (Kadam, 2002). Recirculating the water has the potential to reduce energy consumption, nutrient loss, and water demand. However, this also incurs a risk of infection and growth inhibition from accumulated pathogenic micro-organisms and refractory organic and inorganic chemicals and residual metabolites from the destroyed algae cells (Lundquist et al., 2010). UV disinfection, powered by solar irradiation, mitigates this risk to an extent and incurs an energy cost of $\$0.0035 \text{ kg}^{-1}$ dry biomass.

Table 6

Based on the assumptions made, the estimated BESP of the algal biomass is $\$0.544 \text{ kg}^{-1}$ (Table 6), equating to $\$0.91 \text{ L}^{-1}$ for the extracted biocrude, based on OPEX. A biofuel BESP below the benchmark of $\$1 \text{ L}^{-1}$ is thus potentially achievable. A minimum production cost of $\$0.55 \text{ kg}^{-1}$ dry biomass has been previously reported (F.G. Acie'n, 2014), very similar to the value calculated in the current study, whereas previously estimated biofuel production costs were around $\$1 \text{ L}^{-1}$ for a facility production of 100,000 kg biomass annually (Chisti, 2007). Although the assumptions made in the Chisti study have been subsequently considered overly optimistic (Davis et al., 2011), more recent cost analyses based on highly optimised conditions have led to BESP estimates of $\$0.55\text{-}0.97 \text{ L}^{-1}$ (Hernández-Calderón et al., 2016). Sensitivity to the specific growth rate μ , as indicated in Figure 6, was exemplified by a $\pm 20\%$ change in μ producing a corresponding $\pm 24\%$ change in the BESP.

8 Conclusions

An analysis of the logistics, technical feasibility and operating costs associated with the large-scale implementation of microalgal culture technology (MCT) has been conducted with specific reference to the Arabian Gulf. The facility was designed to provide combined biofixation of CO_2 from flue gas and pollutant removal from wastewaters. The analysis included unit operation selection for fully harnessing the solar energy supply for both algal growth and wastewater disinfection, and maximizing utility of the wastewater supply through recycling. A model developed to simulate CO_2 fixation and nutrient removal was validated using relevant literature data and used to optimise the operating conditions. The impact of the design on temperature regulation was also considered.

The analysis indicated a break-even selling price of $\$0.544 \text{ kg}^{-1}$ for the dried algal biomass required to cover all operating costs under optimum operational conditions. This figure included $\$0.086$ of amounts credited from pollution abatement from reduced emissions. The cost is comparable with that from previous published studies, and the study also corroborated the previously reported sensitivity to the algal growth rate.

Whilst the results appear encouraging, the capital costs associated with implementation and the logistics associated with conveying the flue gas and wastewater to the site should not be overlooked. However, the potential for sustainability associated with the innately reliably high levels of natural light of the Gulf region appear to provide auspicious circumstances for large-scale implementation of MCT. Moreover, extending the assessment to a full life cycle analysis would almost certainly demonstrate the benefits of the scheme in terms of carbon footprint, rather than economics alone.

9 Acknowledgments

This work was made possible by the support of a National Priorities Research Programme (NPRP) grant from the Qatar National Research Fund (QNRF), grant reference number NPRP 6-1436-2-581. The statements made herein are solely the responsibility of the authors.

10 References

- Abdallah, A., Martinez, D., Figgis, B., El Daif, O., 2016. Performance of Silicon Heterojunction Photovoltaic modules in Qatar climatic conditions. *Renewable Energy* 97, 860-865.
- Agulló-Barceló, M., Polo-López, M.I., Lucena, F., Jofre, J., Fernández-Ibáñez, P., 2013. Solar Advanced Oxidation Processes as disinfection tertiary treatments for real wastewater: Implications for water reclamation. *Applied Catalysis B: Environmental* 136-137, 341-350.
- Al-Khayat, J.A., Jones, D.A., 1999. A Comparison of the Macrofauna of Natural and Replanted Mangroves in Qatar. *Estuarine, Coastal and Shelf Science* 49, 55-63.
- Al-Naimi, J.A.S.a.I.S., 2002. Trace Metals in Wastewater Ponds in Qatar. *Qatar Univ. Sci. J* (2002), 22 : 97- 106
- Almomani, F., Al Ketife, A., Judd, S., Shurair, M., Bhosale, R.R., Znad, H., Tawalbeh, M., 2019a. Impact of CO₂ concentration and ambient conditions on microalgal growth and nutrient removal from wastewater by a photobioreactor. *Science of The Total Environment* 662, 662-671.
- Almomani, F., Judd, S., Bhosale, R.R., Shurair, M., Aljaml, K., Khraisheh, M., 2019b. Intergraded wastewater treatment and carbon bio-fixation from flue gases using *Spirulina platensis* and mixed algal culture. *Process Safety and Environmental Protection* 124, 240-250.
- Almomani, F., Judd, S., Shurair, M., 2017. Potential use of mixed indigenous microalgae for carbon dioxide bio-fixation and advanced wastewater treatment, Environmental Division 2017 - Core Programming Area at the 2017 AIChE Spring Meeting and 13th Global Congress on Process Safety AIChE San Antonio, TX, pp. 58-64.
- AlMomani, F.A., Örmeci, B., 2016. Performance Of *Chlorella Vulgaris*, *Neochloris Oleoabundans*, and mixed indigenous microalgae for treatment of primary effluent, secondary effluent and centrate. *Ecological Engineering* 95, 280-289.
- Almomani, F.A., Delatolla, R., Örmeci, B., 2014. Field study of moving bed biofilm reactor technology for post-treatment of wastewater lagoon effluent at 1°C. *Environmental Technology (United Kingdom)* 35, 1596-1604.
- Al Momani, F., Gonzalez, O., Sans, C., Esplugas, S., 2004. Combining photo-Fenton process with biological sequencing batch reactor for 2,4-dichlorophenol degradation, *Water Science and Technology*, pp. 293-298.
- Amanor-Boadu, V., Pfromm, P.H., Nelson, R., 2014. Economic feasibility of algal biodiesel under alternative public policies. *Renewable Energy* 67, 136-142.

- Amoah, P., Drechsel, P., Abaidoo, R.C., Klutse, A., 2007. Effectiveness of common and improved sanitary washing methods in selected cities of West Africa for the reduction of coliform bacteria and helminth eggs on vegetables. *Tropical Medicine & International Health* 12, 40-50.
- Andersen, R.A., 2005. *Algal culturing techniques*. Elsevier Academic Press, Burlington, MA.
- Anderson, D., Glibert, P., Burkholder, J., 2002. Harmful algal blooms and eutrophication: Nutrient sources, composition, and consequences. *Estuaries* 25, 704-726.
- Andruleviciute, V., Makareviciene, V., Skorupskaite, V., Gumbyte, M., 2014. Biomass and oil content of *Chlorella* sp., *Haematococcus* sp., *Nannochloris* sp. and *Scenedesmus* sp. under mixotrophic growth conditions in the presence of technical glycerol. *Journal of Applied Phycology* 26, 83-90.
- Ashghal-PWA, 2014. Public Works Authority Apply Sustainable Developments Concept with Sewerage Works, Qatar.
- Beal, C., Hebner, R., Webber, M., Ruoff, R., Frank Seibert, A., 2012. The Energy Return on Investment for Algal Biocrude: Results for a Research Production Facility.
- Becker, E.W., 2007. Micro-algae as a source of protein. *Biotechnology Advances* 25, 207-210.
- Benemann, J.R., Oswald, W.J., 1996. Systems and economic analysis of microalgae ponds for conversion of CO₂ to biomass. Final report. ; California Univ., Berkeley, CA (United States). Dept. of Civil Engineering, p. Medium: ED; Size: 214 p.
- Bernard, O., Hadj-Sadok, Z., Dochain, D., Genovesi, A., Steyer, J.P., 2001. Dynamical model development and parameter identification for an anaerobic wastewater treatment process. *Biotechnology and Bioengineering* 75, 424-438.
- Borowitzka, M.A., 2005. Culturing microalgae in outdoor ponds. Book Chapter, School of Biological Sciences and Biotechnology.
- Breeze, P., 2016. *Solar Power Generation*.
- Briskin, D.P., 2000. Medicinal Plants and Phytochemicals. Linking Plant Biochemistry and Physiology to Human Health. *Plant Physiology* 124, 507-514.
- Cabello, J., Morales, M., Revah, S., 2014. Dynamic photosynthetic response of the microalga *Scenedesmus obtusiusculus* to light intensity perturbations. *Chemical Engineering Journal* 252, 104-111.
- Cairns, W.L.a.J.M., 1996. New advances in ultraviolet light disinfection technology. WEAO Technical Symposium, Toronto, Ontario.
- Camp, D.M., Spring Creek, 1997. CSO Disinfection Pilot Study. AWPCP Upgrade, Final Report, New York, New York.
- Castillo, A.B., Al-Maslamani, I., Obbard, J.P., 2016. Prevalence of microplastics in the marine waters of Qatar. *Marine Pollution Bulletin* 111, 260-267.
- Chisti, Y., 2007. Biodiesel from microalgae. *Biotechnology Advances* 25, 294-306.
- Corporation, D., 2018. *Dryers*
- Craggs, R., Park, J., Heubeck, S., Sutherland, D., 2014. High rate algal pond systems for low-energy wastewater treatment, nutrient recovery and energy production. *New Zealand Journal of Botany* 52, 60-73.
- Das, P., Thaher, M.I., Hakim, M., Al-Jabri, H.M.S.J., Alghasal, G.S.H.S., 2016. A comparative study of the growth of *Tetraselmis* sp. in large scale fixed depth and decreasing depth raceway ponds. *Bioresource Technology* 216, 114-120.
- Davis, R., Aden, A., Pienkos, P.T., 2011. Techno-economic analysis of autotrophic microalgae for fuel production. *Applied Energy* 88, 3524-3531.

- Davis, R., Markham, J., Kinchin, C., Grundl, N., Tan, E.C.D., Humbird, D., 2016. Process Design and Economics for the Production of Algal Biomass: Algal Biomass Production in Open Pond Systems and Processing Through Dewatering for Downstream Conversion, United States.
- Davis, R.E., Fishman, D.B., Frank, E.D., Johnson, M.C., Jones, S.B., Kinchin, C.M., Skaggs, R.L., Venteris, E.R., Wigmosta, M.S., 2014. Integrated Evaluation of Cost, Emissions, and Resource Potential for Algal Biofuels at the National Scale. *Environmental Science & Technology* 48, 6035-6042.
- Delrue, F., Setier, P.A., Sahut, C., Cournac, L., Roubaud, A., Peltier, G., Froment, A.K., 2012. An economic, sustainability, and energetic model of biodiesel production from microalgae. *Bioresource Technology* 111, 191-200.
- Duffie, J.A., Beckman, W.A., 2013. *Solar Engineering of Thermal Processes*, 4th Edition. John Wiley & Sons.
- E Wiley, P., Campbell, J., McKuin, B., 2011. Production of Biodiesel and Biogas from Algae: A Review of Process Train Options.
- F.G. Acie'n, J.M.F.n., E. Molina-Grima, 2014. Economics of Microalgae Biomass Production, Biofuels from Algae. 2014 Elsevier B.V., Department of Chemical Engineering, University of Almeri'a, Almeri'a, Spain.
- Godwin, A.D., 2017. Indiana Wastewater Treatment Plant Installs Evoqua UV system
WaterWorld Magazine
- Guccione, A., Biondi, N., Sampietro, G., Rodolfi, L., Bassi, N., Tredici, M.R., 2014. *Chlorella* for protein and biofuels: from strain selection to outdoor cultivation in a Green Wall Panel photobioreactor. *Biotechnology for Biofuels* 7, 2-29.
- Hernández-Calderón, O.M., Ponce-Ortega, J.M., Ortiz-del-Castillo, J.R., Cervantes-Gaxiola, M.E., Milán-Carrillo, J., Serna-González, M., Rubio-Castro, E., 2016. Optimal Design of Distributed Algae-Based Biorefineries Using CO₂ Emissions from Multiple Industrial Plants. *Industrial & Engineering Chemistry Research* 55, 2345-2358.
- Hoffman, J., Pate, R.C., Drennen, T., Quinn, J.C., 2017. Techno-economic assessment of open microalgae production systems. *Algal Research* 23, 51-57.
- Huesemann, M., Chavis, A., Edmundson, S., Rye, D., Hobbs, S., Sun, N., Wigmosta, M., 2018. Climate-simulated raceway pond culturing: quantifying the maximum achievable annual biomass productivity of *Chlorella sorokiniana* in the contiguous USA. *Journal of Applied Phycology* 30, 287-298.
- Huntley, M.E., Johnson, Z.I., Brown, S.L., Sills, D.L., Gerber, L., Archibald, I., Machesky, S.C., Granados, J., Beal, C., Greene, C.H., 2015. Demonstrated large-scale production of marine microalgae for fuels and feed. *Algal Research* 10, 249-265.
- Ishika, T., Moheimani, N.R., Bahri, P.A., 2017. Sustainable saline microalgae co-cultivation for biofuel production: A critical review. *Renewable and Sustainable Energy Reviews* 78, 356-368.
- Jazzar, S., Quesada-Medina, J., Olivares-Carrillo, P., Marzouki, M.N., Acie'n-Fernández, F.G., Fernández-Sevilla, J.M., Molina-Grima, E., Smaali, I., 2015. A whole biodiesel conversion process combining isolation, cultivation and in situ supercritical methanol transesterification of native microalgae. *Bioresource Technology* 190, 281-288.
- Jiménez-Pérez, M.V., Sánchez-Castillo, P., Romera, O., Fernández-Moreno, D., Pérez-Martínez, C., 2004. Growth and nutrient removal in free and immobilized planktonic green algae isolated from pig manure. *Enzyme and Microbial Technology* 34, 392-398.

- Jones, S.B., Zhu, Y., Anderson, D.B., Hallen, R.T., Elliott, D.C., Schmidt, A.J., Albrecht, K.O., Hart, T.R., Butcher, M.G., Drennan, C., Snowden-Swan, L.J., Davis, R., Kinchin, C., 2014. Process Design and Economics for the Conversion of Algal Biomass to Hydrocarbons: Whole Algae Hydrothermal Liquefaction and Upgrading. ; Pacific Northwest National Lab. (PNNL), Richland, WA (United States), p. Medium: ED; Size: 69 p.
- Judd, S.J., 2017. Membrane technology costs and me. *Water Research* 122, 1-9.
- Judd, S.J., Al Momani, F.A.O., Znad, H., Al Ketife, A.M.D., 2017. The cost benefit of algal technology for combined CO₂ mitigation and nutrient abatement. *Renewable and Sustainable Energy Reviews* 71, 379-387.
- Jupsin, H., Praet, E., L Vassel, J., 2003. Dynamic mathematical model of high rate algal ponds (HRAP).
- Kadam, K.L., 2002. Environmental implications of power generation via coal-microalgae cofiring. *Energy* 27, 905-922.
- Kim, J., Lee, J.-Y., 2016. Optimal use of Na₂CO₃ buffer for enhanced autotrophic growth of *Nannochloris* sp. and CO₂ bioremediation. *Process Biochemistry* 51, 2162-2169.
- Laboratory, N.E.T., 2010. Carbon Dioxide Enhanced Oil Recovery: Untapped Domestic Energy Supply and Long Term Carbon Storage Solution, Pittsburgh, PA. U.S Department of Energy
- Lam, M.K., Lee, K.T., 2014. Cultivation of *Chlorella vulgaris* in a pilot-scale sequential-baffled column photobioreactor for biomass and biodiesel production. *Energy Conversion and Management* 88, 399-410.
- Lardon, L., Helias, A., Sialve, B., Steyer, J.-P., Bernard, O., 2009. Life-cycle assessment of biodiesel production from microalgae. ACS Publications.
- Laumb, J.D., Kay, J.P., Holmes, M.J., Cowan, R.M., Azenkeng, A., Heebink, L.V., Hanson, S.K., Jensen, M.D., Letvin, P.A., Raymond, L.J., 2013. Economic and Market Analysis of CO₂ Utilization Technologies – Focus on CO₂ derived from North Dakota lignite. *Energy Procedia* 37, 6987-6998.
- Leduy, A., Therien, N., 1979. Cultivation of *spirulina* maxima in an annular photochemical reactor. *The Canadian Journal of Chemical Engineering* 57, 489-495.
- Li, J., Xu, N.S., Su, W.W., 2003. Online estimation of stirred-tank microalgal photobioreactor cultures based on dissolved oxygen measurement. *Biochemical Engineering Journal* 14, 51-65.
- Li, S., Xu, J., Chen, J., Chen, J., Zhou, C., Yan, X., 2014. The major lipid changes of some important diet microalgae during the entire growth phase. *Aquaculture* 428, 104-110.
- Liao, Q., Sun, Y., Huang, Y., Xia, A., Fu, Q., Zhu, X., 2017. Simultaneous enhancement of *Chlorella vulgaris* growth and lipid accumulation through the synergy effect between light and nitrate in a planar waveguide flat-plate photobioreactor. *Bioresource Technology* 243, 528-538.
- Liu, Z., Zhang, F., Chen, F., 2013. High throughput screening of CO₂-tolerating microalgae using GasPak bags. *Aquatic Biosystems* 9, 23.
- Ltd, G.S.E.C., 2017. Parabolic Trough Solar Collector.
- Lundquist, T.J., Woertz, I.C., Quinn, N., Benemann, J.R., 2010. A realistic technology and engineering assessment of algae biofuel production. *Energy Biosciences Institute*, 1.

- M. Raees, A., Ben-Hamadou, R., 2015. Characterization of microalgae species from Qatar coastal waters for animal feed production. Qatar University / Graduate Studies/ College of Art and Sciences.
- Malato, S., Fernández-Ibáñez, P., Maldonado, M.I., Blanco, J., Gernjak, W., 2009. Decontamination and disinfection of water by solar photocatalysis: Recent overview and trends. *Catalysis Today* 147, 1-59.
- McGuigan, K.G., Conroy, R.M., Mosler, H.-J., Preez, M.d., Ubomba-Jaswa, E., Fernandez-Ibañez, P., 2012. Solar water disinfection (SODIS): A review from bench-top to roof-top. *Journal of Hazardous Materials* 235-236, 29-46.
- Meher, L.C., Vidya Sagar, D., Naik, S.N., 2006. Technical aspects of biodiesel production by transesterification—a review. *Renewable and Sustainable Energy Reviews* 10, 248-268.
- Mohamad, S., Fares, A., Judd, S., Bhosale, R., Kumar, A., Gosh, U., Khreisheh, M., 2017. Advanced wastewater treatment using microalgae: effect of temperature on removal of nutrients and organic carbon. *IOP Conference Series: Earth and Environmental Science* 67, 012032.
- Muller, J., and Lem, W. , 2011. UV disinfection of storm water flows and low UVT wastewaters. *IUVA News* 13(3) 13-17.
- Mutanda, T., Ramesh, D., Karthikeyan, S., Kumari, S., Anandraj, A., Bux, F., 2011. Bioprospecting for hyper-lipid producing microalgal strains for sustainable biofuel production. *Bioresource Technology* 102, 57-70.
- Norsker, N.-H., Barbosa, M.J., Vermuë, M.H., Wijffels, R.H., 2011. Microalgal production — A close look at the economics. *Biotechnology Advances* 29, 24-27.
- Orfield, N.D., Keoleian, G.A., Love, N.G., 2014. A GIS based national assessment of algal bio-oil production potential through flue gas and wastewater co-utilization. *Biomass and Bioenergy* 63, 76-85.
- Perry, R.H., 2008. Perry's chemical engineers' handbook.
- Programme, I.g.g.R.D., 2000. Leading options for the capture of CO₂ emissions at power stations.
- Qadir, M., Wichelns, D., Raschid-Sally, L., McCornick, P.G., Drechsel, P., Bahri, A., Minhas, P.S., 2010. The challenges of wastewater irrigation in developing countries. *Agricultural Water Management* 97, 561-568.
- Qatar, S.o., 2013. State of Qatar Ministry of Development Planning and Statistics - Environment Statistics Annual Report
- Qatar, S.o., 2014. Environment Statistics Annual Report
- Rafferty, K.D., Culver, G., 1998. Chapter 11. Heat Exchangers. ; Geo-Heat Center, Klamath Falls, Oregon.
- Raven, J.A., Geider, R.J., 1988. Temperature and algal growth. *New Phytologist* 110, 441-461.
- Rodolfi, L., Chini Zittelli, G., Bassi, N., Padovani, G., Biondi, N., Bonini, G., Tredici, M.R., 2009. Microalgae for oil: Strain selection, induction of lipid synthesis and outdoor mass cultivation in a low-cost photobioreactor. *Biotechnology and Bioengineering* 102, 100-112.
- Saadaoui, I., Al Ghazal, G., Bounnit, T., Al Khulaifi, F., Al Jabri, H., Potts, M., 2016. Evidence of thermo and halotolerant *Nannochloris* isolate suitable for biodiesel production in Qatar Culture Collection of Cyanobacteria and Microalgae. *Algal Research* 14, 39-47.
- Sciandra, A., 1986. Study and modelling of a simple planktonic system reconstituted in an experimental microcosm. *Ecological modelling* 34, 61-82.

- Secretariat, G., 2005. Bulletin of Employment, Wages and Working Hours in: Design and Editing communications Development incorporated, W., DC. (Ed.). General Secretariat for development Planning
- Shah, Y.T., Kelkar, B.G., Godbole, S.P., Deckwer, W.-D., 1982. Design parameters estimations for bubble column reactors. *AIChE Journal* 28, 353-379.
- Shamim Ahmad, K.H. Javed, M.Murad, 1989. Full Scale Performance of Primary Settling Tanks. *Engineering Journal of Qatar University* Vol. 2, 1989.
- Shurair, M.S., Fares Almomani, Simon Judd, Rahul R. Bhosale, Kumar, A., 2016. Potential for green algae *spirulina* to capture carbon dioxide from gas stream. *Materials for Energy, Efficiency and Sustainability: TechConnect Briefs* 2016, 141-143.
- Slade, R., Bauen, A., 2013. Micro-algae cultivation for biofuels: Cost, energy balance, environmental impacts and future prospects. *Biomass and Bioenergy* 53, 29-38.
- Smith, R.A., 1980. The theoretical basis for estimating phytoplankton production and specific growth rate from chlorophyll, light and temperature data. *Ecological Modelling* 10, 243-264.
- Statista, 2016. The Statistics Portal - Qatar - Statistics & Facts.
- Statistics, M.o.D.P.a., 2017. Water statistics in the state of Qatar, 2015.
- Statistics, S.o.Q.-M.o.D.P.a., 2013. Environment Statistics Annual Report
- Stepan, E., Enascuta, C.-E., Opreescu, E.-E., Radu, E., Radu, A., Galan, A.-M., Vasilievici, G., Lavric, V., Velea, S., 2016. Intermediates for synthetic paraffinic kerosene from microalgae. *Fuel* 172, 29-36.
- Stewart, K.M., 2005. The Lakes Handbook Volume 2, Lake Restoration and Rehabilitation Edited By Patrick O'sullivan and Colin s. . *Environmental Conservation* 32, 279-280.
- Sun, A., Davis, R., Starbuck, M., Ben-Amotz, A., Pate, R., Pienkos, P.T., 2011. Comparative cost analysis of algal oil production for biofuels. *Energy* 36, 5169-5179.
- Takagi, M., Watanabe, K., Yamaberi, K., Yoshida, T., 2000. Limited feeding of potassium nitrate for intracellular lipid and triglyceride accumulation of *Nannochloris* sp. UTEX LB1999. *Applied Microbiology and Biotechnology* 54, 112-117.
- Teo, C.L., Idris, A., Zain, N.A.M., Taisir, M., 2014. Synergistic effect of optimizing light-emitting diode illumination quality and intensity to manipulate composition of fatty acid methyl esters from *Nannochloropsis* sp. *Bioresource Technology* 173, 284-290.
- Terigar, B.G., Theegala, C.S., 2014. Investigating the interdependence between cell density, biomass productivity, and lipid productivity to maximize biofuel feedstock production from outdoor microalgal cultures. *Renewable Energy* 64, 238-243.
- Touati, F., Chowdhury, N., Benhmed, K., Gonzales, A., Jr., A. Al-Hitmi, M., Benammar, M., Gastli, A., Ben-Brahim, L., 2017. Long-term performance analysis and power prediction of PV technology in the State of Qatar.
- Toze, S., 2006. Reuse of effluent water—benefits and risks. *Agricultural Water Management* 80, 147-159.
- Turton, R.a.B., R.C. and Whiting, W.B., 1998. Analysis, synthesis and design of chemical processes.
- Vasudevan, V., Stratton, R.W., Pearlson, M.N., Jersey, G.R., Beyene, A.G., Weissman, J.C., Rubino, M., Hileman, J.I., 2012. Environmental Performance of Algal Biofuel Technology Options. *Environmental Science & Technology* 46, 2451-2459.

- Wahidin, S., Idris, A., Shaleh, S.R.M., 2013. The influence of light intensity and photoperiod on the growth and lipid content of microalgae *Nannochloropsis* sp. *Bioresource Technology* 129, 7-11.
- Watanabe, K., Fujii, K., 2016. Isolation of high-level-CO₂-preferring *Picochlorum* sp. strains and their biotechnological potential. *Algal Research* 18, 135-143.
- Weidenfeller, B., Höfer, M., Schilling, F.R., 2004. Thermal conductivity, thermal diffusivity, and specific heat capacity of particle filled polypropylene. *Composites Part A: Applied Science and Manufacturing* 35, 423-429.
- WHO, 2006. Guidelines for the Safe Use of Wastewater, Excreta and Greywater. Vol. 2: Wastewater Use in Agriculture.
- Wileman, A., Ozkan, A., Berberoglu, H., 2012. Rheological properties of algae slurries for minimizing harvesting energy requirements in biofuel production. *Bioresource technology* 104, 432-439.
- Wojtenko, I., K. Stinson, M., Field, R., 2001. Challenges of Combined Sewer Overflow Disinfection by Ultraviolet Light Irradiation.
- Zhu, Y., Albrecht, K.O., Elliott, D.C., Hallen, R.T., Jones, S.B., 2013. Development of hydrothermal liquefaction and upgrading technologies for lipid-extracted algae conversion to liquid fuels. *Algal Research* 2, 455-464.
- Znad, H., Al Ketife, A.M.D., Judd, S., 2018a. Enhancement of CO₂ biofixation and lipid production by *Chlorella vulgaris* using coloured polypropylene film. *Environmental Technology*, 1-7.
- Znad, H., Al Ketife, A.M.D., Judd, S., AlMomani, F., Vuthaluru, H.B., 2018b. Bioremediation and nutrient removal from wastewater by *Chlorella vulgaris*. *Ecological Engineering* 110, 1-7.

List of Tables

Table 1: Reported most influential key operational parameters on algal growth parameters of microalgae *Nannochloris*. sp.

Table 2: Design and operating APR parameters

Table 3: Water and gas concentrations used for calibration, along with source data

Table 4: Numerical values of model parameters

Table 5: Numerical values of model parameters used for validation (Fig. 5)

Table 6: Cost parameter values

Table 1: Reported most influential key operational parameters on algal growth parameters of microalgae *Nannochloris. sp.*

System Config.	Cultiv. media	TN_{in} , mg L ⁻¹	TP_{in} , mg L ⁻¹	TC_{init} , mg L ⁻¹	COD_{init} , mg L ⁻¹	Salinity g L ⁻¹	pH -	Light int, μE	Inlet CO ₂ C _{cg} , % v/v	T, °C	P_X , g L ⁻¹ d ⁻¹	RE TP, %	RE TN, %	μ , d ⁻¹	X_{max} g L ⁻¹	Ref.
Btc.	F/2	nr	nr	nr	nr	40	7-8	100 ^a	3	30	0.05-0.04	nr	nr	0.09-0.18	0.4-0.8	(M. Raees and Ben-Hamadou, 2015)
Btc.	Ss	nr	nr	nr	nr	nr	8.2	50 100 200	nr	23	nr	nr	nr	0.299 0.268 0.299	nr	(Wahidin et al., 2013)
Btc.	BBM	240	50	nr	nr	0.025	8-9	120	nr	20	nr	0.8	3.5	nr	nr	(Jiménez-Pérez et al., 2004)
Btc.	BM	130	20	nr	nr	29	8	150	nr	30	nr	nr	nr	nr	2.6	(Takagi et al., 2000)
Btc.	BG11 & glyc	240	7	2.2	4-120 ^d	0.03	7.6	250	nr	22	0.08 ^b , 0.19 ^c	nr	nr	0.13 ^d - 0.22 ^c	1.78- 1.96	(Andruleviciute et al., 2014)
Btc.	F/2	30	6	120	6	35-40	7 ^e	257±11	99.9 ^e	30	nr	100	96	0.3	2.1	(Kim and Lee, 2016)
Btc. ^f	AM	233	30	nr	nr	nr	8	200	Nr ^g	23	0.16	100	99	nr	2.2	(Jazzar et al., 2015)
CC ^f								950		20 ^f	0.26 ^h	96	93	nr	~1.6	

Btc. batch process; CC continuous process; BBM Blod's Basel Medium; BM Basic medium; BG11 Blue green medium; HRT hydraulic residence time; MWw municipal wastewater; nr Not reported; ^ared & blue system used; ^bsterilized sea water mixed with marine medium, ^dCOD calculated based on glycerol concentration. ^dAutotrophic, ^eMixtrophic, ^gequivalent to removal of 90% of nutrients in MWw, ^e CO₂ gas was bubbled frequently to control pH at 7, Whereas pH initial value was 9, AM algal medium, ^f the cultivation process was maintained at 20°C by circulating thermostaed waster through PBR water jacket, g CO₂ gas was injected on demand, h 0.16 L d⁻¹ was used a dilution rate.

Table 2: Design and operating APR parameters

Variable	Units	Value
Target annual biomass production	tn	4×10^4
Target annual biofuel production	L y ⁻¹	19×10^6
APR reactor (pond) surface area	ha	1
Total area requirement, incl. inoculation system	ha	300
Average daily algal biomass productivity	g dry biomass L ⁻¹	0.5
	tn dry biomass ha ⁻¹ d ⁻¹	0.38
Average annual algal biomass productivity	tn ha ⁻¹ y ⁻¹	133 ^a
Algal bio-crude fraction	wt%	0.5
Oil density	kg m ⁻³	880
Recovery faction	%	95

^aBased on 350 days of operation per year

Table 3: Water and gas concentrations used for calibration, along with source data

No	TN, mg L ⁻¹	TP, mg L ⁻¹	IC, mg L ⁻¹	OC, mg L ⁻¹	I ₀ , μE	T, °C	C _{cg} , (%)	Refs
P1	240	36	3	3.2	100	40	99.9	(Saadaoui et al., 2016))
P2	75	5	4	2.8	100	30	3	(M. Raees and Ben-Hamadou, 2015)
P3	30	5.5	119	2.5	257±11.7	30	99.9	(Kim and Lee, 2016)
P4	240	7	2.2	50	240	25	5	(Liao et al., 2017)

TN Total nitrogen; TP Total phosphorus; IC inorganic carbon; OC Organic carbon; I₀ incident light; C_{cg} CO₂ gas concentration.

Table 4: Numerical values of model parameters^a

Parameter	Units	Estimated value
μ_{max}	d ⁻¹	1
K_n	mg L ⁻¹	0.5
K_p	mg L ⁻¹	0.34
K_c	mg L ⁻¹	0.093×10^2
K_{oc}	mg L ⁻¹	7.83
K_{ih}	mg L ⁻¹	53.8×10^2
I_s	μE m ⁻² s ⁻¹	16
Y_n	-	7×10^{-1}
Y_p	-	9.9×10^{-1}
Y_c	-	9.9×10^{-1}
Y_{OC}	-	1.14×10^{-2} ,
Y_{O2}	-	0.534, (Li et al., 2003)
n	-	0.12
d_{th}	d ⁻¹	9×10^{-2}
k_c	d ⁻¹	5×10^{-1}
D_c	m ² s ⁻¹	14.7×10^{-9} , (Raven and Geider, 1988)
D_o	m ² s ⁻¹	8.0×10^{-9} , (Raven and Geider, 1988)
K_L	g m ⁻²	15
K_s	mg L ⁻¹	7.83
f_p	d	Hours 6 to hours 19
I_d	μE m ⁻² s ⁻¹	4×10^2
$H_{e,C}$	-	8.23×10^{-1} , (Perry, 2008)
$H_{e,O}$	-	3.2×10^{-2} , (Perry, 2008)

^aParameters used in mathematical model for biomass and nutrients

Table 5: Numerical values of model parameters used for validation (Fig. 5)

No	TN, <i>mg L⁻¹</i>	TP, <i>mg L⁻¹</i>	IC, <i>mg L⁻¹</i>	OC, <i>mg L⁻¹</i>	<i>I₀</i> , <i>μE</i>	T, °C	<i>C_{eg}</i> , (%)	Refs
P1	240	7	2.4	40	250	25	0.034	(Andruleviciute et al., 2014)
P2	31	4.11	560	5.5	257	25	12	

Table 6: Cost parameter values

Term	Cost, <i>\$.kg⁻¹</i> dry biomass	Notes	Refs
<u>Cost items used in MCT</u>			
<i>In_{Co}</i> , cost of inoculation	0.36	Calculated, current study: cost of inoculum based GWP design	(Guccione et al., 2014; Norsker et al., 2011; Rodolfi et al., 2009)
<i>Dfg_{Co}</i> , cost of delivered flu gas	0.02	Calculated, current study: based on 52% carbon content in algal dry biomass	(Laboratory, 2010)
<i>Cf_{Co}</i> , cost of cultivation	0.09	Calculated, current study: APR mixing costs	(Norsker et al., 2011)
<i>Ab_{Co}</i> , cost of abiotic treatment	0.012	Calculated, current study: includes filtration.	(Judd, 2017)
<i>Dis_{Co}</i> , cost of disinfection	0.0035	Calculated, current study: based on 35 Wh.m ⁻² for full wastewater disinfection.	(Muller, 2011)
<i>WW_{Co}</i> , cost of delivered WW	0.04	Calculated, current study: water conveyancing.	(Sun et al., 2011)
<i>Sd_{Co}</i> , cost of solar drying	0.012	Calculated, current study: based on energy required for cell harvesting.	(Norsker et al., 2011)
<i>HTL_{Co}</i> , cost of biocrude production	0.00401 ^a	Calculated, current study: assumed 50% conversion factor	(Zhu et al., 2013)
<i>Lab_{Co}</i> , cost of labour	0.088	Estimated, based on literature information for staffing levels and local labour costs	(Hoffman et al., 2017; Secretariat, 2005)
TOTAL OUTGOINGS	0.630		
<u>Credit items used in MCT</u>			
<i>C_{Cr}</i> , credit from carbon removal	0.003 ^b	Estimated, current study	
<i>RN_{Cr}</i> , credit form N removal	0.03 ^c	Estimated, current study	
<i>RP_{Cr}</i> , credit form P removal	0.025 ^c	Estimated, current study	
<i>Fg_{Cr}</i> , credit from flue gas fixation	0.025 ^b	Estimated, current study	
<i>Ae_{Cr}</i> , Aeration energy credit for flue gas	0.0019	Estimated, current study: calculated based on data in reference	(Orfield et al., 2014)
<i>BOD_{Cr}</i> , credit from BOD removed	0.0009 ^d	Calculated, based on 50% removal efficiency	(Craggs et al., 2014)
TOTAL CREDIT	0.086		
NET OPEX	0.544		

Based on electricity market price of 0.11 kWh⁻¹ (Ashghal-PWA, 2014) and currency conversion of 0.274 USD:QAR;

^bcalculated, cf. average value for carbon capture using standard MEA amine scrubbing technology reported as 0.04 \$.kg⁻¹ (Benemann and Oswald, 1996; programme, 2000); ^c based on BOD removal cost 1.48 \$.kg⁻¹ (Davis et al., 2011). ^dbased on 2% BOD removal efficiency.

List of figures

Figure 1: Number of studies undertaken within different subject areas, *Nannochloris. sp.*

Figure 2: Schematic diagram of wastewater pre-treatment, disinfection, and MCT processes used in TEA model.

Figure 3: Model strategy

Figure 4: Computed dynamic performance with respect to algal cell concentration and nutrient removal for wastewater quality and operating conditions of (a) P1, (b) P2, (c) P3 and (d) P4 (Table 3).

Figure 5: Computed dynamic performance with respect to algal cell concentration and nutrient removal for wastewater quality and operating conditions of (a) P1, and (b) P2 (Table 8).

Figure 6: Impact of key parameters on σX , the proportional change in a selected parameter for a. 25% change in parameter X.

Figure 7: Experimentally determined vs. theoretically predicted biomass concentration over range of conditions indicated in Table 8: $R^2 = 0.99$, $P = 0.0001$ and $p > F = < 0.0001$ (i.e. significant). Dashed curved lines indicate >95% confidence bands; dashed horizontal lines represent mean of the Y leverage residuals (measurement of agreement with the model).

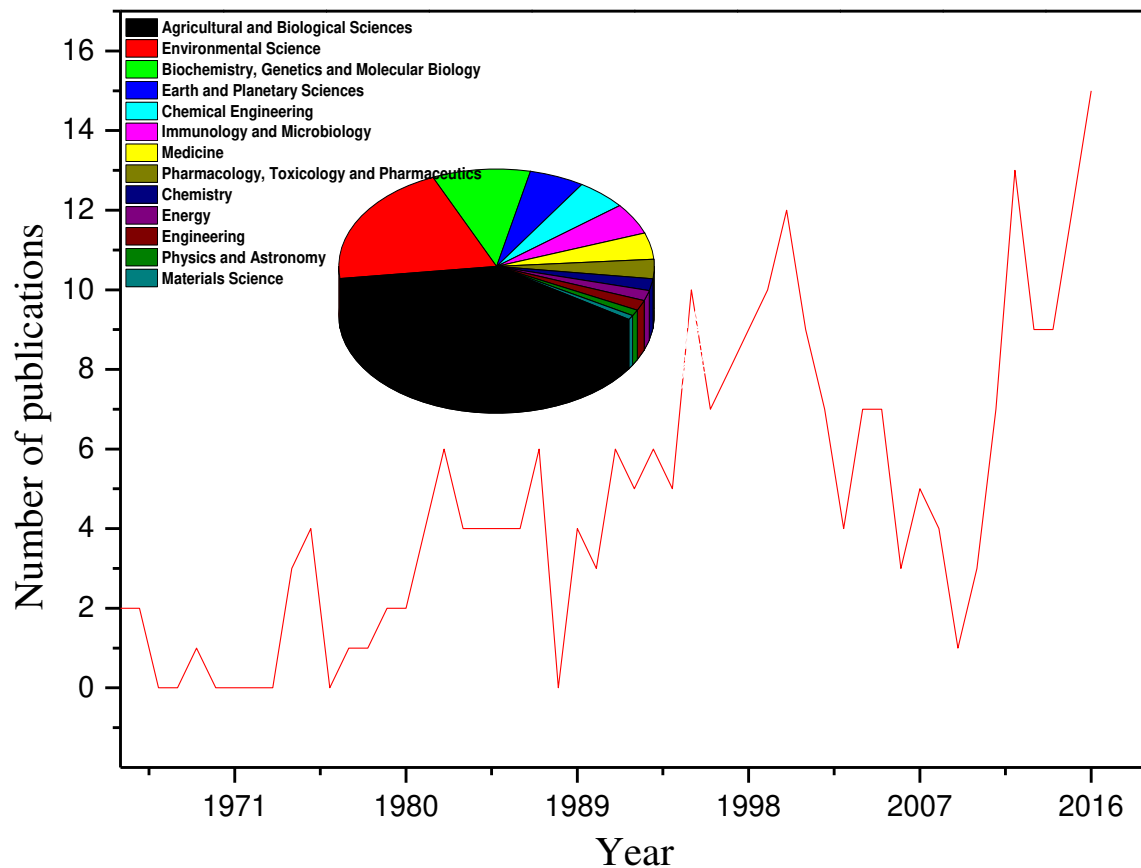


Figure 1: Number of studies undertaken within different subject areas, *Nannochloris*. sp. (SCOPUS database, search term “Nannochloris” for the period between 1965 and 2018).

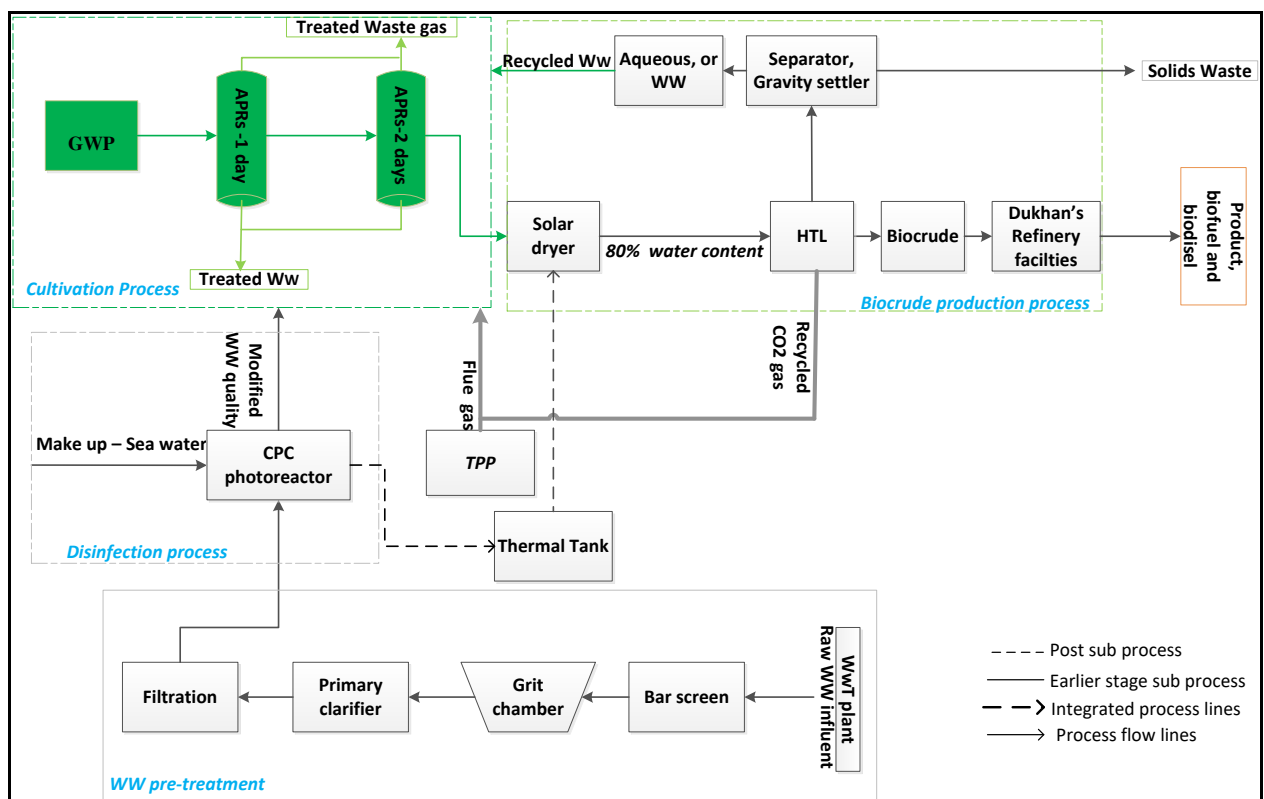


Figure 2: Schematic diagram of wastewater pre-treatment, disinfection, and MCT processes used in model.

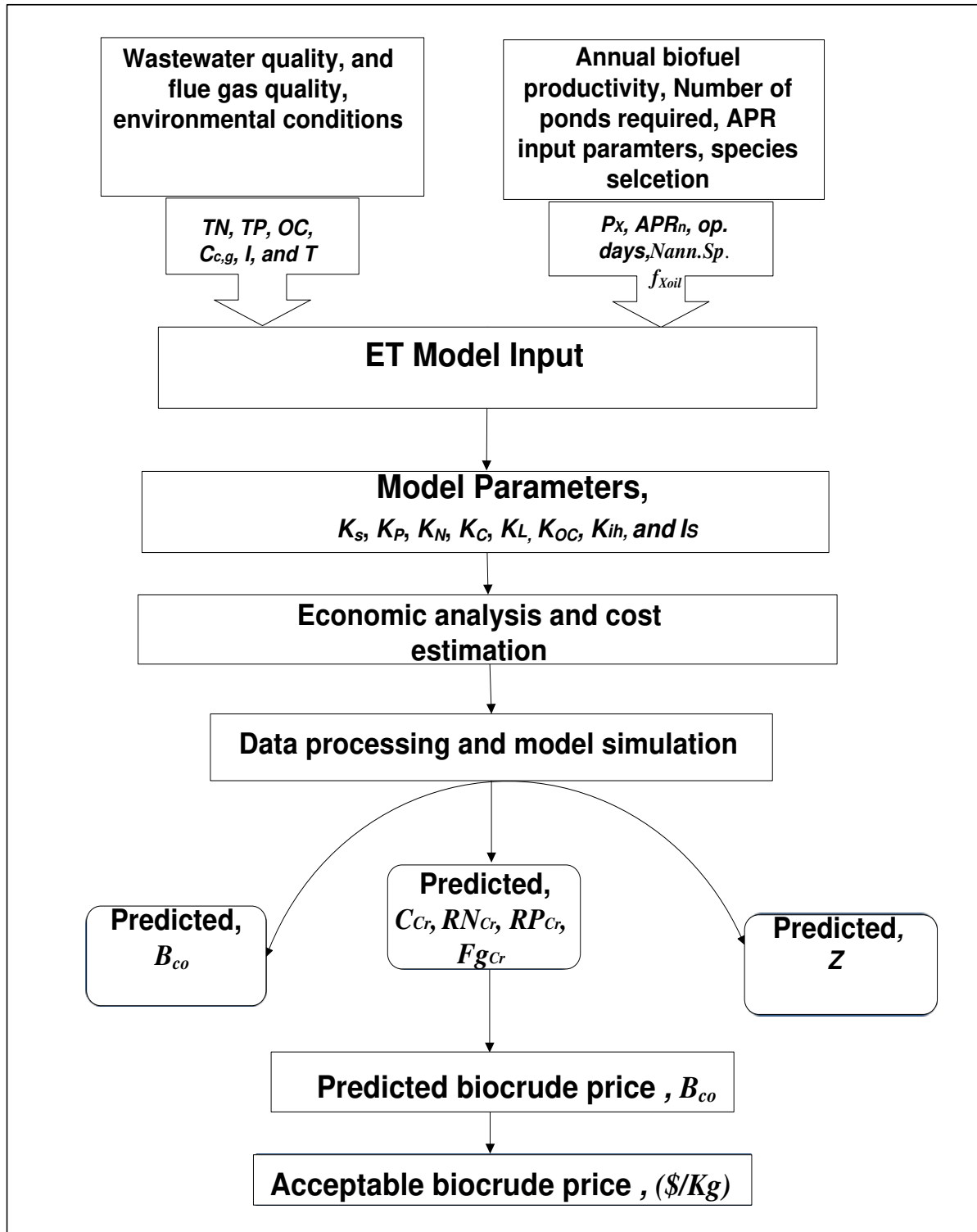


Figure 3: Model strategy

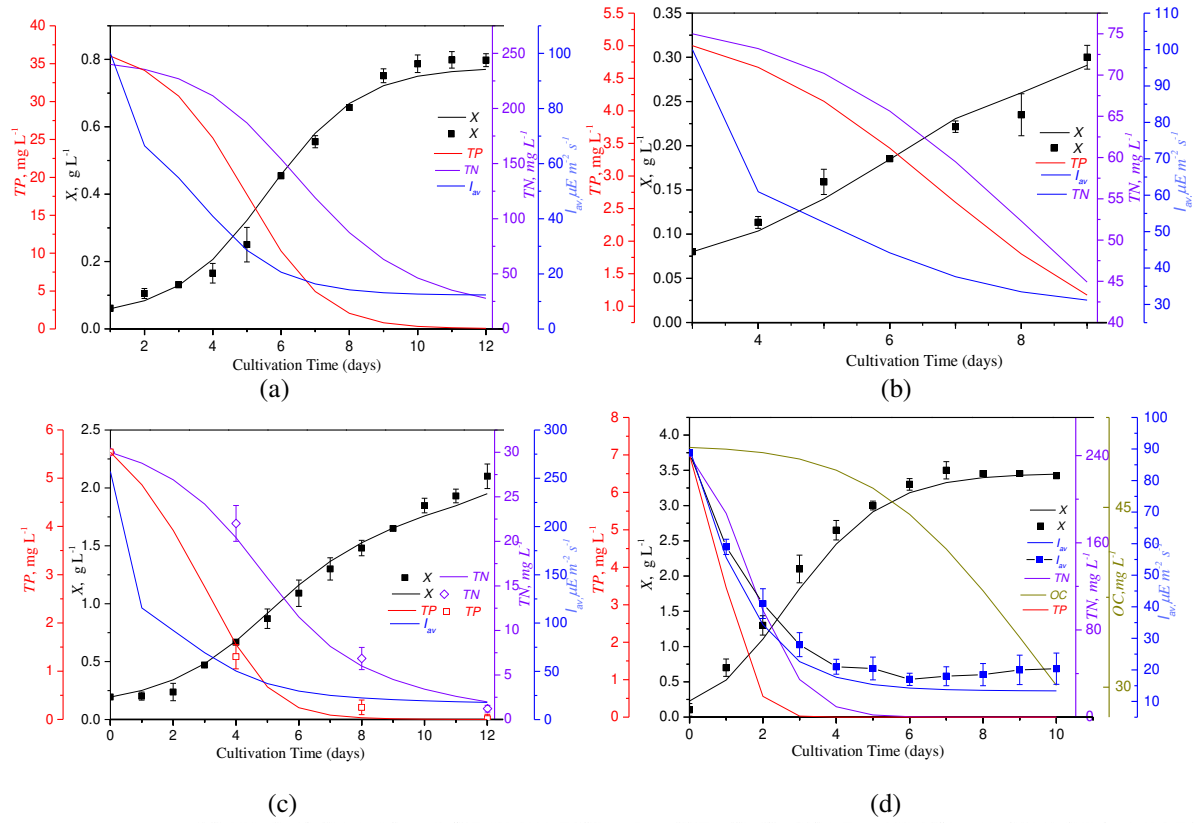


Figure 4: Computed dynamic performance with respect to algal cell concentration and nutrient removal for wastewater quality and operating conditions of (a) P1, (b) P2, (c) P3 and (d) P4 (Table 3).

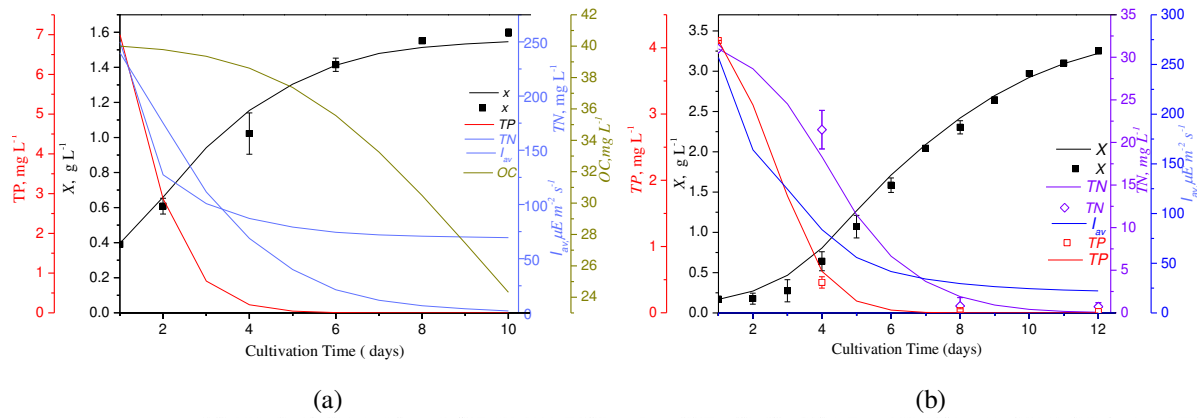


Figure 5: Computed dynamic performance with respect to algal cell concentration and nutrient removal for wastewater quality and operating conditions of (a) P1, and (b) P2 (Table 5).

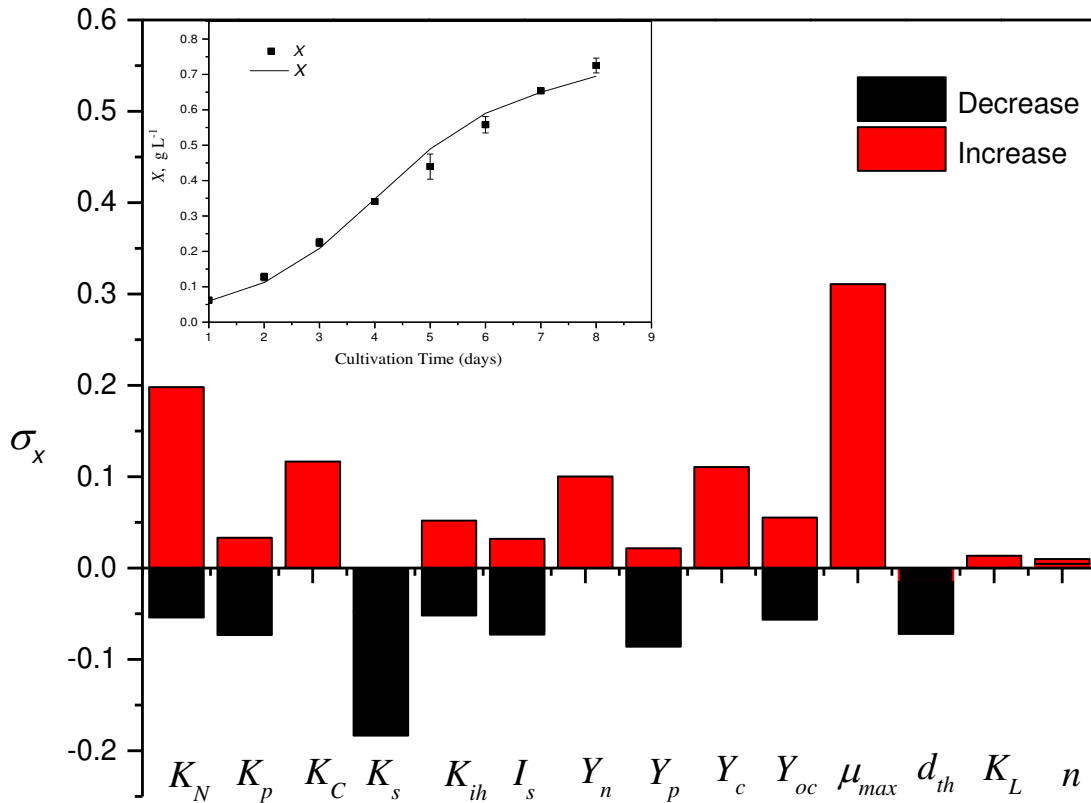


Figure 6: Impact of key parameters on σ_X , the proportional change in a selected parameter for a 25% change in parameter X .

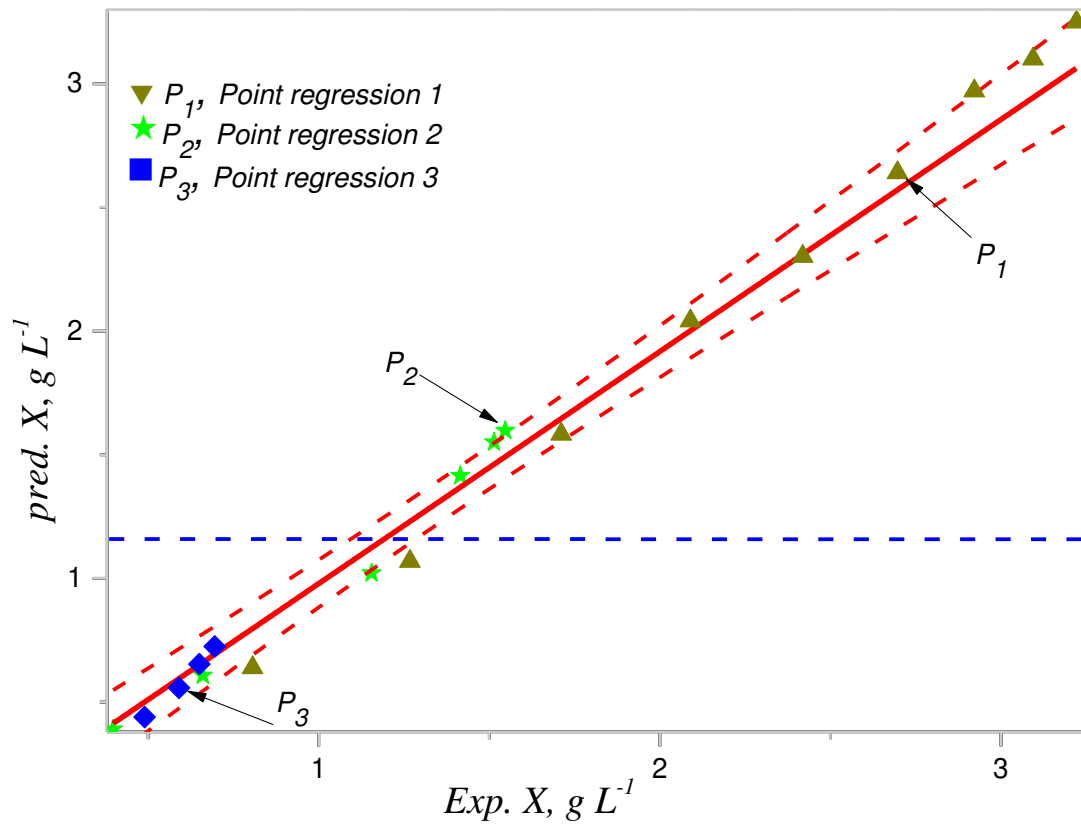


Figure 7: Experimentally determined vs. theoretically predicted biomass concentration over range of conditions indicated in Table 8: $R^2 = 0.99$, $P = 0.0001$ and $p > F = < 0.0001$ (i.e. significant). Dashed curved lines indicate >95% confidence bands; dashed horizontal lines represent mean of the Y leverage residuals (measurement of agreement with the model)

A technoeconomic assessment of microalgal culture technology implementation for combined wastewater treatment and CO₂ mitigation in the Arabian Gulf

Al Ketife, Ahmed M. D.

2019-05-07

Attribution-NonCommercial-NoDerivatives 4.0 International

Al Ketife AM, Almomani F, Muftah EN, Judd S. (2019) A technoeconomic assessment of microalgal culture technology implementation for combined wastewater treatment and CO₂ mitigation in the Arabian Gulf. *Process Safety and Environmental Protection*, Volume 127, July 2019, pp. 90-102

<https://doi.org/10.1016/j.psep.2019.05.003>

Downloaded from CERES Research Repository, Cranfield University